

Monitoring cashew seedlings during interactions with the fungus *Lasiodiplodia theobromae* using chlorophyll fluorescence imaging

C.R. MUNIZ^{*,+}, F.C.O. FREIRE^{*}, F.M.P. VIANA^{*}, J.E. CARDOSO^{*}, C.A.F. SOUSA^{**}, M.I.F. GUEDES^{***}, R. VAN DER SCHOOR[#], and H. JALINK[#]

Embrapa Agroindústria Tropical, Rua Dra. Sara Mesquita, 2270 - Planalto do Pici, 60.511-110, Fortaleza, Ceará, Brazil^{*}

Embrapa Meio-Norte, Av. Duque de Caxias, 5650, 64.006-220, Teresina, Piauí, Brazil^{**}

Universidade Estadual do Ceará, Centro de Ciência da Saúde, Av. Paranjana, 1700, Fortaleza, Ceará, Brazil^{***}

Wageningen UR Greenhouse Horticulture, Droevedaalsesteeg 1, P.O. Box 644, 6700 AP, Wageningen, The Netherlands[#]

Abstract

The chlorophyll (Chl) fluorescence imaging technique was applied to cashew seedlings inoculated with the fungus *Lasiodiplodia theobromae* to assess any disturbances in the photosynthetic apparatus of the plants before the onset of visual symptoms. Two-month-old cashew plants were inoculated with mycelium of *L. theobromae* isolate Lt19 or Lt32. Dark-adapted and light-acclimated whole plants or previously labelled, single, mature leaf from each plant were evaluated weekly for Chl fluorescence parameters. From 21 to 28 days, inoculation with both isolates resulted in the significantly lower maximal photochemical quantum yield of PSII (F_v/F_m) than those for control samples, decreasing from values of 0.78 to 0.62. In contrast, the time response of the measured fluorescence transient curve from dark-acclimated plants increased in both whole plants and single mature leaves in inoculated plants compared with controls. The F_v/F_m images clearly exhibited photosynthetic perturbations 14 days after inoculation before any visual symptoms appeared. Additionally, decays in the effective quantum yield of PSII photochemistry and photochemical quenching coefficient were also observed over time. However, nonphotochemical quenching increased during the evaluation period. We conclude that F_v/F_m images are the effective way of detecting early metabolic perturbations in the photosynthetic apparatus of cashew seedlings caused by gummosis in both whole plants and single leaves and could be potentially employed in larger-scale screening systems.

Additional key words: *Anacardium occidentale*; gummosis; plant disease detection; high-throughput screening.

Introduction

Cashew tree (*Anacardium occidentale* L.) growing in Brazil is focused primarily on producing cashew nuts for the export market. It occupies an area of 760,110 ha, located almost exclusively in the north-eastern region of the country (IBRAF 2011). Brazilian production of cashew nuts exceeded 100,000 t in 2010, yielding US\$ 229.6

million in revenues (IBGE 2011).

Cashew production has been facing some problems, including distressful diseases and pests. The annual production of cashew nuts in Brazil suffered undesirable fluctuations and competed with the top producers: Vietnam, India, Nigeria, the Ivory Coast, and Indonesia

Received 5 September 2013, accepted 24 March 2014.

⁺Corresponding author; phone: +55(85)33917354, e-mail: celli.muniz@embrapa.br, cellimuniz@gmail.com

Abbreviations: Chl – chlorophyll; F_0 – minimal Chl fluorescence of dark-acclimated plants; F_0' – minimum fluorescence during light exposure treatment; F_m – maximal Chl fluorescence of dark-acclimated plants; F_v/F_m – maximal photochemical quantum yield of PSII; F_m' – maximal fluorescence during light treatment; F_v – variable fluorescence; LED – light-emitting diode; NPQ – nonphotochemical fluorescence quenching; Q_A – quinone A; qp – coefficient of photochemical fluorescence quenching; Φ_{PSII} – effective quantum yield of PSII photochemistry; τ_{TR} – time response of the measured fluorescence transient curve from dark-acclimated plants.

Acknowledgments: We would like to thank CAPES (Coordenação de Aperfeiçoamento de Pessoal de Nível Superior) for granting scholarships through the “Adding value to Brazilian Tropical fruits: MIPS (Multiple Imaging Plant Stress) and TRS (Time Resolved Spectroscopy) applications to assure uniform quality of papaya and mango” project, coordinated by Dr. H. Filgueiras and Dr. M. Teixeira de Souza Junior for his support through Embrapa LABEX Europe.

(FAOSTAT 2011). Among the problems that negatively affect the cashew tree and compromise cashew nut production is gummosis, a disease, caused by the fungus *Lasiodiplodia theobromae* (Pat.) Griff. & Maubl., a member of the family Botryosphaeriaceae. It is an endophytic fungus able to colonize its hosts without obvious symptoms but significantly reducing the yield of cashews (Cardoso *et al.* 2009; Muniz *et al.* 2011).

It is estimated that half a million early dwarf cashew seedlings are produced annually in the Brazilian Northeast (Cavalcanti Junior *et al.* 2002). Once infected, cashew seedlings constitute a primary inoculum for the fungus in the field and usually display no visual symptoms of infection. Therefore, the lack of an early detection method contributes to the spread of the disease (Cardoso *et al.* 2010). Thus far, diagnosis and identification of the gummosis pathogen has been based upon the emergence of symptoms and subsequent isolation of the pathogen on agar media. However, a major problem with visual assessment of infected plants is the difficulty of this delayed observation and in the interpretation of the initial symptoms, which requires an expert eye. By this point, plants and even orchards might be seriously compromised. An early and noninvasive detection method would enhance the screening of problematic plants, especially at nurseries. High-throughput approaches for screening multiple-diseased plants have gained much attention, especially for fungal diseases (Scholes and Rolfe 2009).

The ratio of F_v/F_m can be used to estimate the maximal quantum yield of the PSII photochemistry. When plants are exposed to abiotic and biotic stresses, decreases in F_v/F_m are frequently observed, and their measurement provides a simple and rapid method of monitoring stress. The parameter refers to measurements with dark-acclimated samples (Oxborough and Baker 1997). When samples are exposed to continuous actinic light or to saturating light pulses, the fluorescence rises from the minimal fluorescence level (F_0'), to the maximal fluorescence level during light treatment, (F_m'). Saturation means light strong enough to fully reduce the electron transport chain so that the PSII becomes closed. If the PSII reaction centres cannot perform photochemical reactions,

then photochemical quenching is equal to zero and maximal fluorescence levels are reached (F_m and F_m' in the dark-acclimated and light-exposed samples, respectively). The difference between F_m' and F_t is designated as F_q' and results from the quenching of F_m' by PSII photochemistry. F_q'/F_m' is also known as Φ_{PSII} and nonphotochemical processes are typically represented as nonphotochemical quenching (NPQ) and assigned to heat dissipation (Bilger and Björkman 1990, Maxwell and Johnson 2000, Roháček 2002, Baker 2008).

Chl fluorescence measurement techniques have been widely used as rapid and noninvasive methods for estimating photosynthetic performance in plants. Improvements in instrumentation and image acquisition (through red fluorescence capture by specific filters) and the development of distinct measuring protocols have enhanced the possibility of visualizing the differences in the responses of plants to biotic stresses in many pathogen systems (Chærle *et al.* 2004, 2007). Changes in Chl fluorescence associated with fungal infections have been widely related and imaging systems have become suitable study tools to investigate these plant-fungus interactions (Scholes and Rolfe 2009).

Cashew plants affected by gummosis show reductions in stomatal conductance and, consequently, in photosynthesis (Bezerra *et al.* 2003). Therefore, if photosynthesis itself is altered, changes in the parameters related to Chl fluorescence are very likely to occur and are detectable by either a fluorescence imaging system or by advanced statistical analysis; in this last case, a more sensitive detection method (Lazar 2006). In this study, we used a fluorescence imaging system that was able to detect both F_0 and F_m and yield an image of F_v/F_m in addition to other Chl fluorescence parameters related to the inoculation of cashew plants with two different strains of *L. theobromae*. The images were analysed to determine the responses of plants prior to the occurrence of visual symptoms. Besides, we tested these imaging techniques on single mature leaves to establish their potential use as an assay for the early and rapid detection of gummosis in cashew seedlings.

Materials and methods

Plants and growth conditions: The cashew seedlings were obtained from seeds of the open-pollinated, dwarf, cashew clone CCP 76, developed by the Brazilian Agricultural Corporation (EMBRAPA). Seeds were placed in pots (15 cm in height) containing a fertilised commercial substrate (*Lentse Potgrond*, The Netherlands). Every 15th d, the plants were supplemented with 1/10 strength Hoagland's nutrient solution (Hoagland and Arnon 1950). Plants were grown in a growth chamber at 25°C, at 60–70% relative humidity with a photoperiod of 12/12 h light/dark cycles, and $180 \pm 20 \mu\text{mol m}^{-2} \text{s}^{-1}$ of PAR.

Fungal isolates of *L. theobromae* originated from infected cashew plant tissue, obtained from the collection maintained by Embrapa Tropical Agroindustry (Table 1).

Experimental design: In the first experiment, two-month-old cashew seedlings were inoculated with mycelium of *L. theobromae*. The inoculum was introduced into the plants through a small hole made in the stem using an electric drill. After inoculation, the hole was covered with tape. Control plants were subjected to the same procedure, but without the introduction of the inoculum. The

Table 1. Fungal isolates, hosts, and collecting site.

Fungal isolate, code	Host collecting site
<i>L. theobromae</i> , Lt19	<i>Anacardium occidentale</i> -gummosis symptoms, São Raimundo Nonato, Piauí state, Brazil
<i>L. theobromae</i> , Lt32	<i>Anacardium occidentale</i> - black branch dieback of cashew, Serra do Mel, Rio Grande do Norte state, Brazil

experimental design was completely randomised with three treatments (plants not inoculated, plants inoculated with *L. theobromae* isolate Lt19, and plants inoculated with *L. theobromae* isolate Lt32) and five replicates. Whole plants or previously labelled, single mature leaves were evaluated every 7th d until 28 d from the inoculation (DAI). For single mature leaves, the same leaf was employed for all measurements. In this experiment, Chl fluorescence parameters were only determined in dark-acclimated plants; the F_v/F_m ratio and the time response for the measured fluorescence transient curve from dark-acclimated plants (τ_{TR}) were the parameters obtained.

The second experiment followed the same procedure except that only *L. theobromae* isolate Lt19 was inoculated into the cashew seedlings. Additionally, the plants were evaluated for a longer time, 50 DAI, and the Chl fluorescence parameters for both dark and light-acclimated plants were determined. F_v/F_m , τ_{TR} , Φ_{PSII} , NPQ, and coefficient of photochemical fluorescence quenching (q_P) were subjected to an analysis of variance (*ANOVA*) for each treatment or for each evaluation period. When the Chl fluorescence parameters reached significant differences ($P=0.05$) within treatments, Tukey's test was performed. In both cases, the 'time zero' measurement was performed before the inoculation procedure.

Chl fluorescence imaging: A home-made, imaging fluorometer was used to obtain the principal Chl fluorescence parameters. It consisted of an array of light emitting diodes (LED), a charge coupled device (CCD) camera, an LED power supply, and software to operate the device and capture the Chl fluorescence images and data. An array of LED lamps generated the saturating light pulses. It consisted of two sets of lamps (each set with 20 small LEDs) mounted on a 30 cm × 30 cm aluminium plate 1 cm thick. The lamps were adjusted to deliver square wave pulses with 15-ms and 14-ms intervals between them. At the level of the plant leaves, 50 cm from the CCD camera, each light flash, for the dark-adapted plants, reached 1,000 $\mu\text{mol}(\text{photon}) \text{ m}^{-2} \text{ s}^{-1}$ in the red spectrum (620 nm). As successive pulses of 30 light flashes were emitted over the plants, saturation of the photochemistry was assured. Fluorescence was detected by a CCD camera that produced 320 × 240 pixel images in the 2×2 binning mode for higher sensitivity using a 14-bit grey scale. For fluorescence detection, the light was filtered by an interference filter mounted between the lens ($f = 8 \text{ mm}$) and the CCD-chip of the camera. The LEDs light source

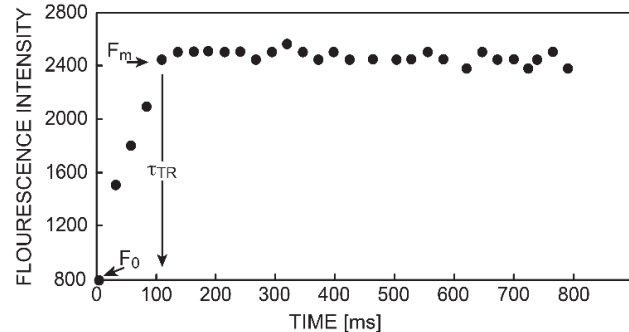


Fig. 1. Illustration of the effects of light saturation on plants showing the major parameters measured from which the images of F_v/F_m and τ_{TR} were constructed. Plants were dark-acclimated for 30 min before being exposed to saturating light for 842 ms. Saturating light was composed of 30 light flash subpulses with 15-ms and 14-ms intervals between them. At the level of plant leaves, at 50 cm from the CCD camera, each subpulse reached $1,000 \mu\text{mol m}^{-2} \text{ s}^{-1}$.

(saturating light pulse and actinic light) and the CCD camera were controlled using *Transient Chlorophyll Fluorescence* (TCF) software written in Delphi. With the LED lamps turned off, a dark image was captured and stored in the computer using the same protocol as for the fluorescence imaging. Soon thereafter, with the LED lamps turned on, 30 pulses of light were emitted over the plants. During each light flash for the 15-ms subpulses, one image was captured by the camera and transferred directly to the computer. After the entire sequence of images, typically 30, the dark image was subtracted from the fluorescence images to eliminate the background signal. This sequence yielded images for which each pixel contained fluorescence time information. The first value at $t = 15 \text{ ms}$ corresponded to the minimal Chl fluorescence from dark-acclimated plants (F_0). The maximal fluorescence value where the curve became saturated corresponded to F_m . Each pixel was fitted to the exponential regression: $F(t) = F_0 + (F_m - F_0)[1 - \exp(-t/\tau_{TR})]$. An estimate of the yield of the PSII photochemistry could be calculated from: $F_v/F_m = (F_m - F_0)/F_m$. This calculation was performed for each pixel, yielding an image for estimating F_v/F_m and an image corresponding to the time response (τ_{TR}) of the photosynthetic system under experimental conditions, which correlated with the time response of the measured fluorescence transient curve (Kautsky induction). In Fig. 1, the time response (τ_{TR}) is perceived as the time interval, in which F_m is reached starting from F_0 .

Table 2. Formulas for the chlorophyll fluorescence parameters.

Chlorophyll fluorescence parameters	Definition
$F_0' = 1/(F_0 - 1/F_m + 1/F_m')$	Minimal chlorophyll fluorescence from light-acclimated plants
$F_v/F_m = (F_m - F_0)/F_m$	Maximal photochemical quantum yield of PSII
$\Phi_{PSII} = (F_m' - F_t)/F_m'$	Effective quantum yield of PSII
$q_P = (F_m' - F_t)/(F_m' - F_0')$	Coefficient of photochemical fluorescence quenching
$NPQ = (F_m - F_m')/F_m'$	Nonphotochemical fluorescence quenching

Measurement protocol: Saturating light was applied to whole plants or to attached, single mature leaves (always the same leaves) that had been previously dark-acclimated for 30 min to obtain the initial parameters for Chl fluorescence, *i.e.*, F_0 and F_m , and τ_{TR} . Plants were then exposed to continuous white actinic illumination ($50 \mu\text{mol m}^{-2} \text{ s}^{-1}$

PAR), with saturating light being applied each minute. At the end of 15 min, data were obtained for transient Chl fluorescence from the light-acclimated plants. The main parameters for Chl fluorescence were calculated according to van Kooten and Snel (1990) (Table 2).

Results

Chl fluorescence parameters obtained in both dark- and light-acclimated cashew seedlings: Initially, the values of the F_v/F_m ratios decreased slightly in controls 7 DAI, but then they recovered. At 14 DAI, the F_v/F_m ratios decreased significantly, but only in the whole plants

inoculated with fungal isolate Lt32 (Fig. 2A). From 21 to 28 DAI, inoculation with both isolates resulted in significantly lower F_v/F_m ratios than in the control samples for the whole plants and the single mature leaves (Fig. 2B). The τ_{TR} from dark-acclimated plants was also altered after fungal inoculation of the cashew seedlings (Figs. 3A,B). In both whole plants and the single mature leaves, there was a trend of increasing τ_{TR} at 21 DAI with *L. theobromae* isolates. The average values of τ_{TR} for the controls were approximately 182 ms for the whole plants and 148 ms for the single mature leaves. After fungal inoculation (Lt19), responses to light were delayed for 232 ms for the single mature leaves and for 256 ms for the whole plants.

Inoculation with isolate Lt19 significantly altered the values of the Chl fluorescence parameters in the whole seedlings when compared with controls (Fig. 4). The inoculated plants showed decreases in the F_v/F_m ratios from 28 DAI (Fig. 4D), confirming the previous decline in the F_v/F_m values over time (Fig. 2A). The lower values for the F_v/F_m ratios, which reached 0.53 and were significantly lower than those in the controls, were observed at 50 DAI, coinciding with the initial appearance of visual symptoms in the plants. The Φ_{PSII} decreased significantly, which was apparent in the inoculated plants compared with controls from the 7 DAI onward (Fig. 4A). At 21 DAI, the q_P (Fig. 4B) began declining and, simultaneously, the NPQ (Fig. 4C) began rising.

Images of the parameter F_v/F_m : The changes after the inoculation of the cashew seedlings with *L. theobromae* (Lt32) on single mature leaves and whole plant samples are presented in Figs. 5 and 6, respectively. Initially, both the infected and control plants showed the high F_v/F_m ratios at time zero according to the colour of their leaves, which can be compared with the colour bar scale. The first presymptomatic indications were observed at 14 DAI. For this treatment, time-evolution images displayed extensive zones of low F_v/F_m values spread over the entire leaf

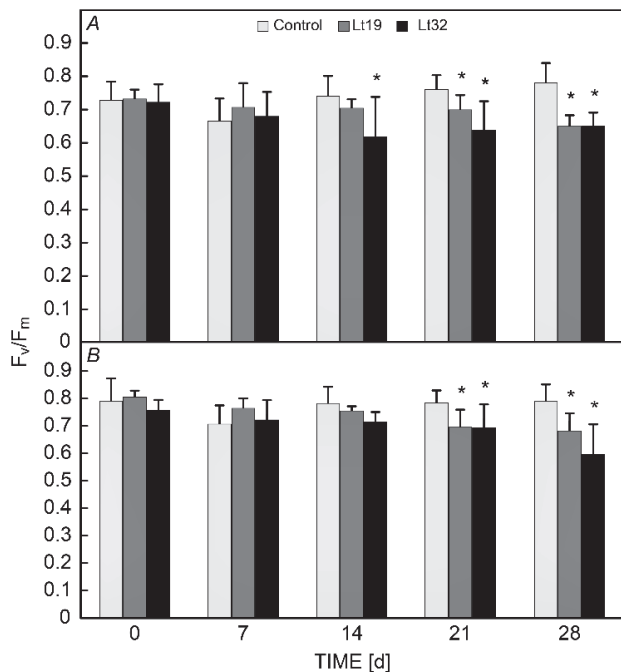


Fig. 2. Time-course analysis of maximum photochemical quantum yield of PSII (F_v/F_m) for whole cashew plants (A) or single mature leaves (B) inoculated with *Lasiodiplodia theobromae* isolates (Lt19 or Lt32). Each value represents the mean \pm SD of five replicates. * – a significant difference from the control at $P < 0.05$. Plants were dark-acclimated for 30 min before being exposed to saturating light for 842 ms. Saturating light was composed of 30 light flash subpulses with 15-ms and 14-ms intervals between them. At the level of plant leaves, at 50 cm from the CCD camera, each subpulse reached $1,000 \mu\text{mol m}^{-2} \text{ s}^{-1}$.

surface; these were first observed as yellow areas and evolved to larger red areas by the end of the experiment, corresponding to much lower F_v/F_m ratios. This behaviour was also noticed for *L. theobromae* (Lt19). The metabolic perturbations were clearly detectable in the images along the borders of leaves, spreading gradually into inner regions and also appearing as red areas. Using the images of Chl fluorescence from the whole cashew plants, we could also observe reductions in the F_v/F_m ratio in the

inoculated plants (Fig. 6) over time. For each plant, some leaves had more pronounced diseased zones than others, and differences in perturbations patterns were clearly visible, depending on the plant and the leaf. After 14 DAI, the first fluorescence-detectable stresses were observed in plants inoculated with both *L. theobromae* isolates to a greater or lesser degree. By that time, visual symptoms were still not apparent in the inoculated plants.

Discussion

The F_v/F_m , Chl fluorescence parameter, is usually in the range of 0.78–0.84 for healthy vascular plants (Björkman and Demmig 1987). If the photosynthetic apparatus is somehow damaged or injured, this value might drop considerably. Chl fluorescence techniques have not been previously reported relating to biotic stresses in cashew plants. The few data on the use of Chl fluorescence in

cashew crops refer to studies in plants under drought and salt stresses, in which the F_v/F_m ratio decreased from 0.80 to 0.65 (Blaikie and Chacko 1998, de Souza *et al.* 2005). The F_v/F_m ratios decays observed in the current study, from approximately 0.80 to 0.60, indicated alterations in the photochemical apparatus of the cashew seedlings.

According to Scholes and Rolfe (2009), Chl fluorescence imaging provides a direct measure of primary plant function; thus, any perturbation caused during plant-fungal interactions can improve the possibility of distinguishing between infected and uninfected tissues. Different pathogen systems, however, lead to a diversity of responses and the interpretation of Chl fluorescence parameters is crucial. The behaviour of these parameters over time is one comprehensive pathway for demonstrating specific responses. In this case, time studies gave us clues about damages to plant physiology following fungal inoculation, even when visual symptoms were not yet accessible.

The slight declines in the F_v/F_m ratios observed in both the whole plant or in the single mature leaf of the controls 7 d after drill perforation might be due to the stress caused by mechanical injury; they were able to recover afterwards. For the *L. theobromae*-inoculated plants, however, significant and continuous reductions in the F_v/F_m ratios over time demonstrated actual perturbations in plant metabolism, as clearly observed in both types of samples. For cashew plants, the pathogenic action of *Lasiodiplodia* is not fully understood, but damage to the plant might be occurring *via* reductions in water and nutrient transport, leading to reduced photosynthesis, which would explain the substantial decreases in the F_v/F_m ratios (Cardoso *et al.* 2010). Previous determinations of the microscopic features of the colonization of cashew plants by *L. theobromae* (Muniz *et al.* 2011) indicated the presence of the fungus within the xylem vessels. In some asymptomatic samples, this presence could certainly allow the provocation of perturbations observed in Chl fluorescence parameters, even before symptoms occurrence, especially in whole plants. The blocking of vascular bundles, within branches and stems, by the fungus would impair the physiological status of the whole plant, not only of a single leaf, leading to higher F_v/F_m ratios for single leaf measurements. Furthermore, disturbances in photosynthetic parameters observed at the end of the experiment

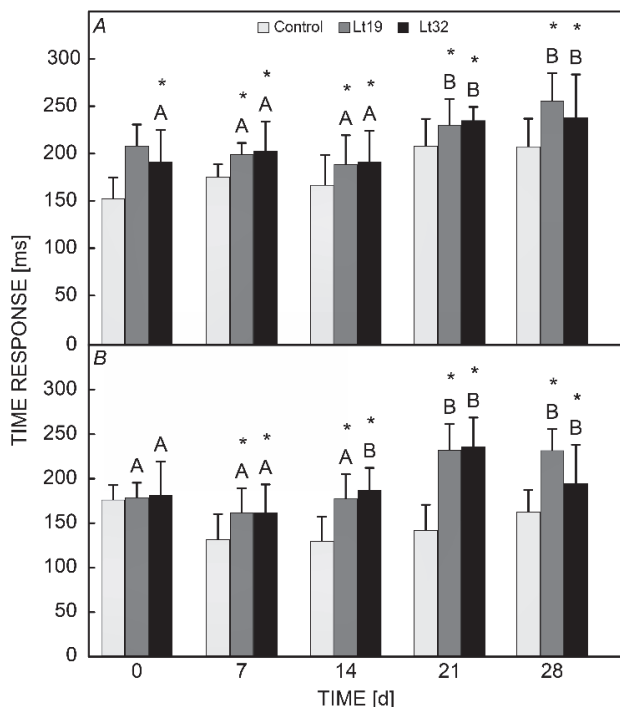


Fig. 3. Time-course analysis of time response of the measured fluorescence transient curve from dark-acclimated plants (TR) for whole cashew plants (A) or single mature leaf (B) inoculated with *Lasiodiplodia theobromae* isolates (Lt19 and Lt32). Each value represents the mean \pm SD of five replicates. Within each treatment, different capital letters show significant differences across days after inoculation periods. * – a significant difference from the control at $P < 0.05$. Plants were dark-acclimated for 30 min before being exposed to saturating light for 842 ms. Saturating light was composed of 30 light flash subpulses with 15-ms and 14-ms intervals between them. At the level of plant leaves, at 50 cm from the CCD camera, each subpulse reached $1,000 \mu\text{mol m}^{-2} \text{s}^{-1}$.

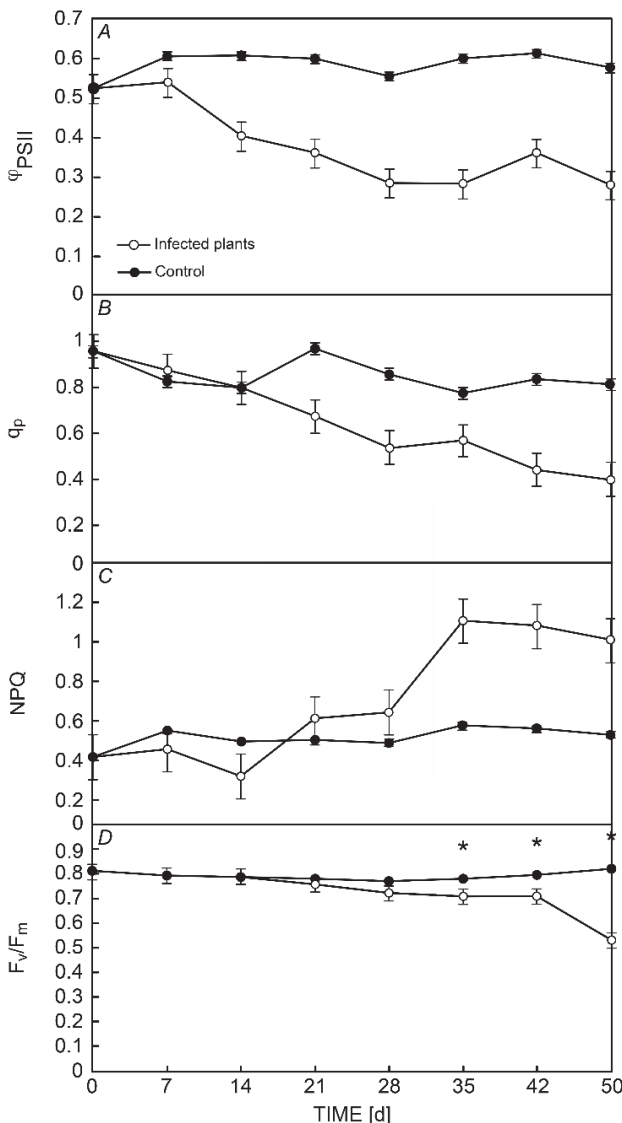


Fig. 4. Effects of the inoculation of the fungus *Lasiodiplodia theobromae* (isolate Lt19) on chlorophyll fluorescence parameters in cashew seedlings using chlorophyll fluorescence imaging technique. (A) PSII effective quantum yield (Φ_{PSII}); (B) photochemical quenching coefficient (qp); (C) nonphotochemical quenching (NPQ); (D) PSII maximum quantum yield (F_v/F_m). Each value represents the mean \pm SD of five replicates. * – a significant difference from the control at $P < 0.05$.

were in total accord with a high degradation of parenchyma cells, with a serious compromise of the inner layers of cell walls, also noticed during ultrastructural investigation of the interaction between *Lasiodiplodia* and cashew plants (Muniz *et al.* 2011). As the distribution of and response to the fungus within the plant tissues can be extremely variable and sometimes unpredictable, a single leaf might not represent the sum of all negative effects. Therefore, heterogeneities in the photosynthetic patterns of leaves are easily revealed, mainly when the fluorescence levels for each pixel can be added and accessed (Nedbal

and Whitmarsh 2004). Additionally, the development of an indirect enzyme-linked immunosorbent assay (ELISA) intended to detect the fungus both *in vitro* and *in planta* (artificially and naturally infected) produced some positive readings for asymptomatic samples (Muniz *et al.* 2012). This observation that both physiological disturbances and fungal distribution were detectable at precocious stages of fungal settlement supports the idea that decreases in F_v/F_m ratios might indicate real perturbations in plant metabolism possibly related to fungal establishment.

One major advantage of the Φ_{PSII} parameter is the possibility of being measured in sunlight, in light-adapted leaves, while the measurement of F_v/F_m requires dark-adaptation of the leaves. In this case, both parameters revealed that plants were suffering after the fungus inoculation. This has also been shown to be true for other Chl fluorescence settlements used as diagnostic tools for the early detection of fungal infections (Cséfalvay *et al.* 2009). In other plant-fungal interactions, Rolfe and Scholes (2010) observed a decline in F_v/F_m , an initial reduction in Φ_{PSII} , and an increase in NPQ. Such results are in agreement with those obtained in this study. It is expected that in stressed plants, energy is dissipated by nonphotochemical processes rather than photochemical ones. Nevertheless, the time interval required for observing these effects and their relationship to the establishment of visible symptoms is largely dependent on multiple factors, such as the metabolites and toxins produced by the pathogen, its mode of nutrition, and differences in the hosts' responses (Wolpert 2002). For instance, in grapes infected with downy mildew (*Plasmopara viticola*), reductions in F_v/F_m and Φ_{PSII} could be detected three days before visible symptoms became apparent and these effects did not extend widely across the entire leaf (Cséfalvay *et al.* 2009). Likewise, tomato plants infected with *Fusarium oxysporum* f.sp. *lycopersici* had their physiological parameters influenced by the fungal inoculation treatment, exhibiting early decreases in Φ_{PSII} and also in qp (Segarra *et al.* 2010). This was also true for lettuce infected by *Bremia lactucae* (Prokopová *et al.* 2010). Chou *et al.* (2000), working on interactions between *Albugo candida* (Pers.) Kuntze and *Arabidopsis thaliana*, showed that as photosynthesis declined in areas directly invaded by fungal mycelium, NPQ increased, indicating that light that was not used for photosynthetic electron transport but it was dissipated by nonphotochemical processes.

Fluorescence images of F_v/F_m showed heterogeneity in the metabolic perturbations to pathogen inoculation spread across plants and leaves and different parts of leaves. Although each pulse light measurement had an intensity of 1,000 $\mu\text{mol}(\text{photon}) \text{ m}^{-2} \text{ s}^{-1}$, the successive 30 flashes of 15-ms subpulses of this light were strong enough to saturate the plant photochemistry. Therefore, the lower F_v/F_m values encountered correlated with the effects of the fungus itself. The magnitude of the different possibilities for host reactions in a plant-pathogen interaction implies

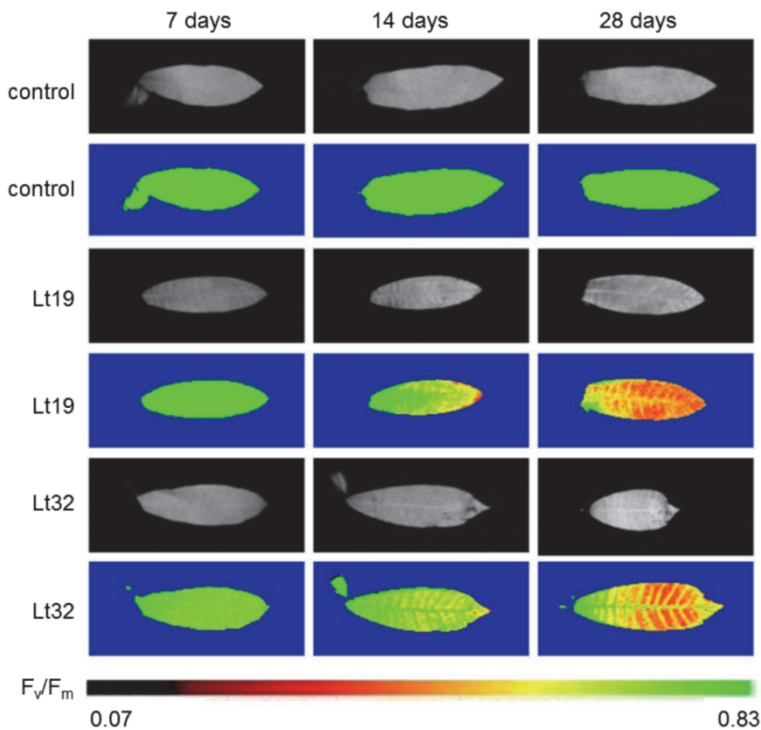


Fig. 5. Images of maximum photochemical quantum yield of PSII (F_v/F_m) for the single mature leaf of cashew seedlings inoculated with *Lasiodiploidia theobromae* using chlorophyll fluorescence imaging technique. Images in rows represent different fungal inoculation treatments: no inoculation (control), inoculation with *L. theobromae* (Lt19) or with *L. theobromae* (Lt32). Images in columns represent the course of time at 7, 14, and 28 days after inoculation. Coloured bar below the images of F_v/F_m show the range of values and how they mapped to the colour palette.

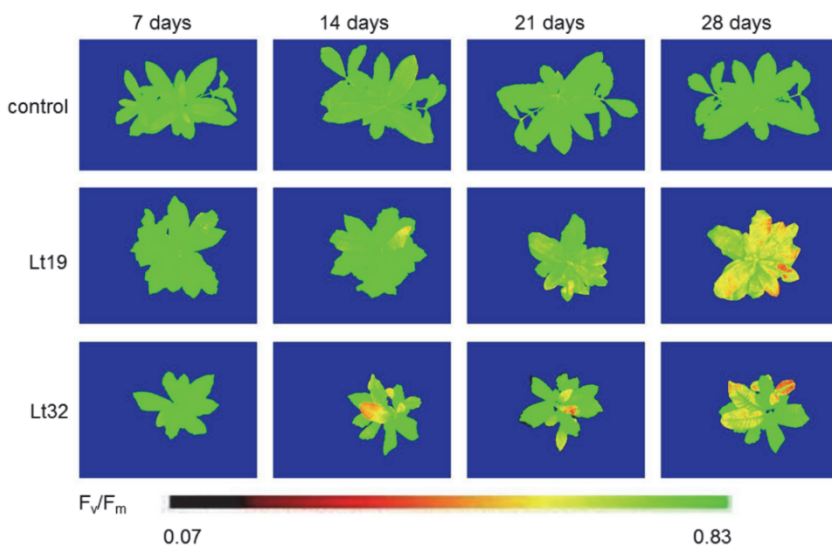


Fig. 6. Images of maximum photochemical quantum yield of PSII (F_v/F_m) for the whole cashew seedlings inoculated with *Lasiodiploidia theobromae* using chlorophyll fluorescence imaging technique. Images in rows represent different fungal inoculation treatments: no inoculation (control), inoculation with *L. theobromae* (Lt19) or with *L. theobromae* (Lt32). Images in columns represent the course of time at 7, 14, 21, and 28 days after inoculation. Coloured bar below the images of F_v/F_m show the range of values and how they mapped to the colour palette.

an intrinsic difficulty in obtaining a single pattern of predictable responses. Variations in the severity of virulence in different *L. theobromae* isolates have been described. Pathogenicity trials conducted by Taylor *et al.* (2005) and Urbez-Torres (2008) with virulent strains showed that the severity of the lesions produced by different isolates differed. It is quite plausible, therefore, to notice differences in fluorescence parameters patterns between distinct fungal cultures. Whatever the type of disarrangement provoked, the sensitivity of Chl fluorescence imaging to very small changes in plant metabolism demonstrates the enormous potential of this technique to provide details about such systems, especially for virulent and aggressive strains. Timing, the location of pathogen

development, and the severity of damage are some examples of parameters being evaluated in current studies (Rolle and Scholes 2010). A number of studies have used Chl fluorescence imaging to detect fungal infection prior to the appearance of visible symptoms. For example, in *A. thaliana* infected with the biotrophic fungus *Albugo candida*, moderate irradiance was tightly correlated with the timing of the appearance of visible symptoms (Chou *et al.* 2000). McElrone *et al.* (2010) found that reductions in Φ_{PSII} in hardwood trees infected by *Phyllosticta* and *Cercospora* extended a few millimetres beyond the visible symptoms of infection. In other interactions, effects might be observed across the entire leaf and extend far beyond the area of visible symptoms. In oat leaves infected with

Puccinia coronata, Scholes and Rolfe (1996) found marked changes in the patterns observed during photosynthetic induction. As the infection progressed, both Φ_{PSII} and NPQ were significantly reduced in the areas of visible symptoms, but Φ_{PSII} was also diminished across the rest of the leaf with a corresponding increase in NPQ. A similar leaf-wide reduction in Φ_{PSII} was found in lupine infected with the necrotroph *Pleiochaeta setose*, although a halo of activity was retained at the symptom margins (Guidi *et al.* 2007). The nutrition and pathogenicity modes of these distinct fungi are markedly variable, but in all cases, reduced patterns of photosynthetic activity have been pronounced, especially as the infection evolved over time.

For cashew plants inoculated with *L. theobromae*, very low F_v/F_m image profiles overlapped with visible symptoms at the end of the experiment. Considering that F_v/F_m is easily affected by any photosynthetic disorder agent and that F_v/F_m can be easily measured, we believe that the integration of this parameter into Chl fluorescence imaging could be recommended for a fast and reliable screening. Images of both whole plants and single mature leaves demonstrated essentially the same Chl fluorescence alterations. Therefore, both screenings could be used in

large-scale efforts, for example, to detect infected plants in a nursery. However, if more precise Chl fluorescence data were needed, the data generated from a single mature leaf measured in the horizontal position were more reliable.

Conclusion: Chl fluorescence imaging was able to detect disturbances in cashew plants inoculated with *L. theobromae* fungi prior to the establishment of symptoms. Distinctions between infected and uninfected tissues could be determined, relying on both Chl fluorescence parameters and images. When we consider the possibility of some *L. theobromae* strains being capable of acting as pathogens, triggering gummosis, and leading to metabolic disorders, it would certainly be possible that first perturbations could be precisely detected using this technique. In seedling nurseries, a mechanism that would be able to collect early informations about disease disturbances could enhance the quality of plants destined for planting. Furthermore, robust automated systems would enlarge the number of samples that would be subjected to screening, supporting the production of cashew plants with a technologically advanced system.

References

Baker, N.R.: Chlorophyll Fluorescence: A probe of photosynthesis *in vivo*. – Annu. Rev. Plant Biol. **59**: 89-113, 2008.

Bezerra, M.A., Cardoso, J.E., Santos, A.A. *et al.*: [Effect of gummosis in the photosynthesis of the precocious dwarf cashew.] – Bol. Pesq. Desenvol. Emb. Agroind. Trop. **8**: 1-12, 2003. [In Portuguese]

Bilger, W., Björkman, O. Role of the xanthophyll cycle in photoprotection elucidated by measurements of light-induced absorbance changes, fluorescence and photosynthesis in leaves of *Hedera canariensis*. – Photosynth. Res. **25**: 173-185, 1990.

Björkman, O., Demmig, B.: Photon yield of O_2 evolution and chlorophyll fluorescence characteristics at 77 K among vascular plants of diverse origins. – Planta **170**: 489-504, 1987.

Blaikie, S.J.; Chacko, E.K.: Sap flow, leaf gas exchange and chlorophyll fluorescence of container-grown cashew (*Anacardium occidentale* L.) trees subjected to repeated cycles of soil drying. – Aust. J. Exp. Agri. **38**: 305-311, 1998.

Cardoso, J.E., Bezerra, M.A., Viana, F.M.P. *et al.*: [Endophyte occurrence of *Lasiodiplodia theobromae* in cashew tissues and its transmission by vegetative propagules.] – Summa Phytopathol. **35**: 262-266, 2009. [In Portuguese]

Cardoso, J.E., Cavalcanti, J.J.V., Cysne, A.Q. *et al.*: [Effect of cashew clone used as rootstocks and scions on gummosis incidence in cashew plants.] – Rev. Bras. Frutic. **32**: 847-854, 2010. [In Portuguese]

Cavalcanti Junior, A.T., Correa, D., Bueno, D.: [Propagation.] – In: Barros, L.M. (ed.): [Cashew production: technical aspects.] Pp. 43-48. Emb. Agroind. Trop., Fortaleza 2002. [In Portuguese]

Chaerle, L., Hagenbeek, D., De Bruyne, E. *et al.*: Thermal and chlorophyll-fluorescence imaging distinguish plant-pathogen interactions at an early stage. – Plant Cell Physiol. **45**: 887-896, 2004.

Chaerle, L., Leinonen, I., Jones, H.G., Van der Straeten, D.: Monitoring and screening plant populations with combined thermal and chlorophyll fluorescence imaging. – J. Exp. Bot. **58**: 773-784, 2007.

Chou, H.M., Bundoock, N., Rolfe, S.A., Scholes, J.D.: Infection of *Arabidopsis thaliana* leaves with *Albugo candida* (white blister rust) causes a reprogramming of host metabolism. – Mol. Plant Pathol. **1**: 99-113, 2000.

Cséfalvay, L., Di Gaspero, G., Matouš, K., Bellin, D., Ruperti, B., Olejníčková, J.: Pre-symptomatic detection of *Plasmopara viticola* infection in grapevine leaves using chlorophyll fluorescence imaging. – Eur. J. Plant Pathol. **125**: 291-302, 2009.

de Souza, R.P., Ribeiro, R.V., Machado, E.C. *et al.*: [Photosynthetic responses of young cashew plants to varying environmental conditions.] – Pesqui. Agropecu. Bras. **40**: 735-744, 2005. [In Portuguese]

FAOSTAT. Rome 2011. Available on <http://faostat.fao.org/>. Access on 17 Mai 2011.

Guidi, L., Mori, S., Degl'Innocenti, E., Pecchia, S.: Effects of ozone exposure or fungal pathogen on white lupin leaves as determined by imaging of chlorophyll a fluorescence. – Plant Physiol. Bioch. **45**: 851-857, 2007.

Hoagland, D.R., Arnon, D.A.: The water-culture method of growing plants without soil. – Circ. Calif. Agr. Exp. Sta. **347**: 1-39, 1950.

IBGE. SIDRA, 2011. [Aggregate database.] Table 1613. Available on <<http://www.sidra.ibge.gov.br/bda/tabela/listab.asp?c=1613&z=t&o=11>>. Access on 9 Nov. 2011. [In Portuguese]

IBRAF, 2011. [Brazilian exportations of processed fruits 2009/2010.] Available on <www.ibraf.org.br/estatisticas/est_processadas.asp>. Access on 9 Nov. 2011. [In Portuguese]

Lazar, D., Susila, P., Naus, J.: Early detection of plant stress from changes in distributions of chlorophyll a fluorescence parameters measured with fluorescence imaging. – J. Fluoresc.

16: 173-176, 2006.

Maxwell, K.; Johnson, G.N. Chlorophyll fluorescence - a practical guide. – *J. Exp. Bot.* **51**: 659-668, 2000.

McElrone, A.J., Hamilton, J.G., Krafnick, A.J. *et al.*: Combined effects of elevated CO₂ and natural climatic variation on leaf spot diseases of redbud and sweetgum trees. – *Environ. Pollut.* **158**: 108-114, 2010.

Muniz, C.R., Freire, F.C.O., Viana, F.M.P. *et al.*: Colonization of cashew plant by *Lasiodiplodia theobromae*: Microscopical features. – *Micron* **42**: 419-428, 2011.

Muniz, C.R., Freire, F.C.O., Viana, F.M.P. *et al.*: Polyclonal antibody-based ELISA in combination with specific PCR amplification of internal transcribed spacer regions for the detection and quantitation of *Lasiodiplodia theobromae*, causal agent of gummosis in cashew nut plants. – *Ann. Appl. Biol.* **160**: 217-224, 2012.

Nedbal, L., Whitmarsh, J.: Chlorophyll fluorescence imaging of leaves and fruits. – In: Papageorgiou, G.C., Govindjee (ed.): *Chlorophyll Fluorescence: a Signature of Photosynthesis* Pp. 279-319. Springer, Dordrecht 2004.

Oxborough, K., Baker, N.R.: Resolving chlorophyll *a* fluorescence images of photosynthetic efficiency into photo-chemical and non-photochemical components-calculation of *qp* and *F_{v'}/F_{m'}* without measuring *F_{0'}*. – *Photosynth. Res.* **54**: 135-142, 1997.

Prokopová, J., Špundová, M., Sedlářová *et al.*: Photosynthetic responses of lettuce to downy mildew infection and cytokinin treatment. – *Plant Physiol. Bioch.* **48**: 716-723, 2010.

Roháček, K.: Chlorophyll fluorescence parameters: the definitions, photosynthetic meaning, and mutual relationships. – Photosynthetica **40**: 13-29, 2002.

Rolfe, S.A., Scholes, J.D.: Chlorophyll fluorescence imaging of plant-pathogen interactions. – *Protoplasma* **247**: 163-175, 2010.

Scholes, J.D., Rolfe, S.A.: Photosynthesis in localised regions of oat leaves infected with crown rust (*Puccinia coronata*): quantitative imaging of chlorophyll fluorescence. – *Planta* **199**: 573-582, 1996.

Scholes, J.D., Rolfe, S.A.: Chlorophyll fluorescence imaging as a tool for understanding the impact of fungal diseases on plant performance: a phenomics perspective. – *Funct. Plant Biol.* **36**: 880-892, 2009.

Segarra, G., Casanova, E., Avilés, M., Trillas, I.: *Trichoderma asperellum* strain T34 controls fusarium wilt disease in tomato plants in soilless culture through competition for iron. – *Microbial Ecol.* **59**: 141-149, 2010.

Taylor, A.; Hardy, G.E.S.; Wood, P.; Burgess, T.: Identification and pathogenicity of *Botryosphaeriaceae* species associated with grapevine decline in Western Australia. – *Australas. Plant Path.* **34**: 187-195, 2005.

Úrbez-Torres, J.R.; Leavitt, G.M.; Guerrero, J.C. *et al.*: Identification and pathogenicity of *Lasiodiplodia theobromae* and *Diplodia seriata*, the causal agents of bot canker disease of grapevines in Mexico. – *Plant Dis.* **92**: 519-529, 2008.

van Kooten, O., Snell, J.F.H.: The use of chlorophyll fluorescence nomenclature in plant stress physiology. – *Photosynth. Res.* **25**: 147-150, 1990.

Wolpert, T.J., Dunkle, L.D., Ciuffetti, L.M.: Host-selective toxins and avirulence determinants: what's in a name? – *Annu. Rev. Phytopathol.* **40**: 251-285, 2002.